Numerical Solutions of Second Elastic-Plastic Fracture Mechanics Parameter in Test Specimens under Biaxial Loading

Ping Ding[1], Xin Wang[1,*]

[1] Department of Mechanical and Aerospace Engineering, Carleton University,
Ottawa, Ontario, K1S 5B6, Canada
*Corresponding author: xwang@mae.carleton.ca

Abstract Extensive finite elements analyses have been conducted to obtain solutions of constraint parameter A, which is the second parameter in a three-term elastic-plastic asymptotic expansion for crack-tip field, for test specimens under biaxial loading. Three mode I plane-strain test specimens, *i.e.* single edge cracked plate (SECP), centre cracked plate (CCP) and double edge cracked plate (DECP) were studied. The crack geometries analysed include shallow to deep cracks, and the biaxial loading ratios analysed are 0.5 and 1.0. Solutions of parameter A were obtained for materials following the Ramberg-Osgood power law with hardening exponents of n=3, 4, 5, 7 and 10. Remote tension loading were applied which covers deformation range from small-scale to large-scale yielding. Based on the finite element results of constraint parameter A, crack-tip constraint effect for cracked specimens under biaxial loading is analysed. Using the relationships between A and other two commonly-used second fracture parameters, Q and A_2, the present solutions for A can be used to calculate parameters Q and A_2.

Keywords elastic-plastic fracture, second fracture parameter, biaxial loading, solutions, constraint effect

1. Introduction

In classical elastic-plastic fracture mechanics (EPFM), one-parameter approach, which describes the HRR fields [1, 2] based on J-integral [3], usually can work well for high constraint cases. For low constraint cases, under high loading conditions, the dominance of J-integral will be lost, and the one-parameter approach of J-integral will not be appropriate any more.

Two-parameter approaches have been developed to overcome the limitation of the EPFM one-parameter approach, in which a second fracture mechanics parameter is introduced to characterize the constraint effect besides the load-related parameter J-integral. Several commonly-used two-parameter approaches are, J-T [4-6], J-Q [7, 8] and J-A_2 (J-A) [9-12] approaches, where constraint parameter A is a different normalizing form of A_2 [11, 12].

Determination of J-integral and second fracture mechanics parameter, T, Q and A_2 (A), is precondition of application of J-T, J-Q and J-A_2 (A) approaches. In the early development of EPFM, J-integral solutions have been well established. The solutions of constraint parameter T-stress have also been well established in the literature. Currently, numerical method, such as finite element analysis (FEA) method, is the main method for the determination of constraint parameters Q and A_2 (A). For example, Nikishkov *et al*. [12] suggested an algorithm which determines solutions of A using a least squares procedure based on the finite element analysis results. Although with high accuracy, numerical method is a time-consuming way to obtain solutions of parameters. Correspondingly, understanding of constraint effect near crack-tip is limited because of the scarcity of solutions of constraint parameter A_2 (A) and Q.

In previous works of authors [13, 14], extensive finite element analyses were conducted to obtain solutions of parameter A for several typical two-dimensional (2D) plane-strain specimens under uniaxial loading conditions. Biaxial loading cases are of equal theoretical and engineering practical significance as uniaxial loading cases. Many researchers have focused their investigations on biaxial loading cases, for example, the results reported by Pop *et al*. [15] and Méité *et al*. [16]. In the present work, solutions for A will be obtained for biaxial loading cases for three mode I crack plane-strain specimens, single edge cracked plate (SECP), center cracked plate (CCP) and double edge cracked plate (DECP). In this work, extensive finite element analyses will be carried out for SECP, CCP and DECP cracked specimens under biaxial loading conditions with biaxial loading

ratios λ=0.5, 1.0, to determine numerical solutions of constraint parameter *A* through a least squares fitting method suggested by Nikishkov *et al*. [12]. Using the obtained numerical solutions of constraint parameter, *A*, constraint effect near crack-tip of specimens is analyzed. Numerical solutions for constraint parameter *A* under biaxial loading conditions obtained in this work can be used to estimate other two commonly-used constraint parameters A_2 and *Q* conveniently by the relationships between *A* and A_2, *Q* presented in authors' previous paper [13].

2. Theoretical background

2.1. *J-A* approach

As mentioned in introduction section, *J-A* two-parameter approach of elastic-plastic fracture mechanics, which is suggested by Nikishkov *et al*. [11, 12], is an alternate format of *J*-A_2 approach developed by Yang *et al.* [9, 10]. In these two formats of the approach, both the constraint parameter *A* and A_2 are the magnitude of the second term in a three-term series expansion of crack-tip stress fields. In this paper, the *J-A* format is used.

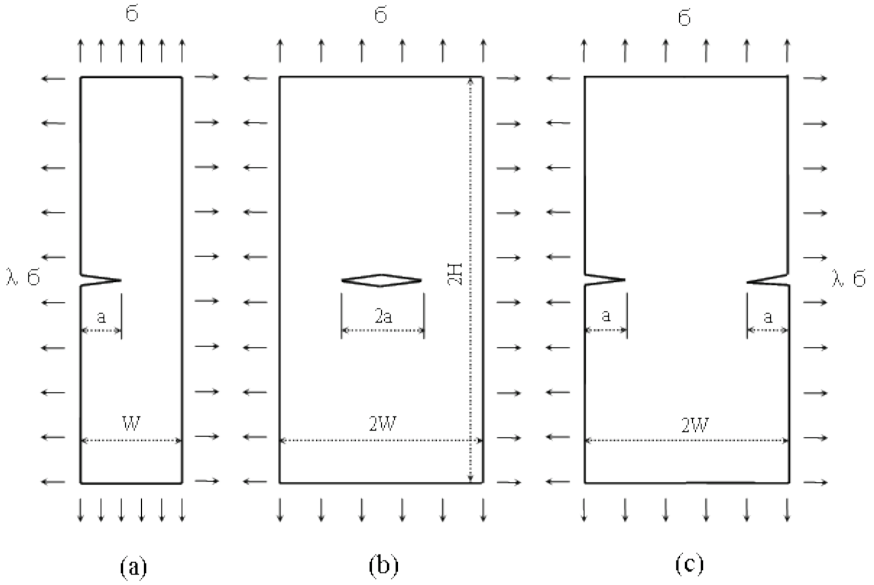

Figure 1. Cracked specimens under biaxial loading: (a) SECP, (b) CCP, (c) DECP

Considering a two-dimensional elastic-plastic specimen containing a mode I crack under plane strain condition, if the elastic-plastic behavior of the specimen material described by deformation theory of plasticity follows the Ramberg-Osgood relationship, the uniaxial stress-strain curve can be described as:

$$\frac{\varepsilon}{\varepsilon_0}=\frac{\sigma}{\sigma_0}+\alpha\left(\frac{\sigma}{\sigma_0}\right)^n \tag{1}$$

where α is a material coefficient, *n* is the hardening exponent ($n > 1$), $\varepsilon_0=\sigma_0/E$, *E* is Yong's modulus, σ is the stress applied on the remote end of specimen, and σ_0 is the material yield stress.

Table 1. Comparison of constraint parameter *Q* for CCP under *a/W*=0.5, *n*=10, λ=0.5

$\log(J/(a\sigma_0))$	-2.900	-2.491	-2.256	-2.074	-1.855	-1.593	-1.299	-0.991
Q_{SSY} [Ref.]	-0.2107	-0.3553	-0.4822	-0.5711	-0.6497	-0.7690	-0.8223	-0.9315
Q_{SSY}	-0.2196	-0.3714	-0.4849	-0.5763	-0.6758	-0.7790	-0.8739	-0.9815
Diff. (%)	4.232	4.526	0.558	0.923	4.003	1.299	6.274	5.376

In the *J-A* two-parameter approach suggested by Nikishkov *et al*. [11, 12], for the hardening exponent $n \geq 3$ and under plane-strain conditions, the three-term asymptotic solution expression for

stress field near the crack-tip in an elastic-plastic material is given as:

$$\frac{\sigma_{ij}}{\sigma_0} = A_0 \bar{r}^s \bar{\sigma}_{ij}^{(0)}(\theta) - A\bar{r}^t \bar{\sigma}_{ij}^{(1)}(\theta) + \frac{A^2}{A_0} \bar{r}^{2t-s} \bar{\sigma}_{ij}^{(2)}(\theta) \tag{2}$$

In Eq. (2), $\sigma_{ij}(\theta)$ are stress components, σ_r, σ_θ and $\sigma_{r\theta}$ in a polar coordinate system with origin at the crack-tip; $\bar{\sigma}_{ij}^{(0)}(\theta), \bar{\sigma}_{ij}^{(1)}(\theta)$ and $\bar{\sigma}_{ij}^{(2)}(\theta)$ are normalized angular stress functions. The dimensionless radius $\bar{r}$ is defined as $\bar{r} = r/(J/\sigma_0)$, where J is the J-integral at the crack-tip. Power t is an eigenvalue depending on the hardening exponent n of Ramberg-Osgood relation, and power $s=-1/(n+1)$. The polynomial coefficient A_0 is defined as [11], $A_0=(\alpha\varepsilon_0 I_n)^{-1/(n+1)}$, where I_n is a scaling integral only depending on n, see Refs. [1, 2]. Nikishkov [11] has proposed a computational algorithm to determine the values of normalized angular functions $\bar{\sigma}_{ij}^{(0)}(\theta)$, $\bar{\sigma}_{ij}^{(1)}(\theta)$, $\bar{\sigma}_{ij}^{(2)}(\theta)$, asymptotic power t, and scaling integral I_n. The three-term expansion in Eq. (2) for the crack-tip stress (displacement) fields is controlled by two parameters, the magnitude of the first term (J-integral) and a second parameter (A) controlling the second and third term.

2.2. Numerical method for determining of constraint parameter

The application of J-A (A_2) two-parameter approach depends on the determination of the load-related parameter J and constraint parameter A (A_2). The solutions of J-integral (including analytical, numerical and approximate solutions) have been well established in the literature, such as the numerical solution of J suggested by Moran and Shih [17], which has been adopted in the commercial code ABAQUS [18] utilized in the present research.

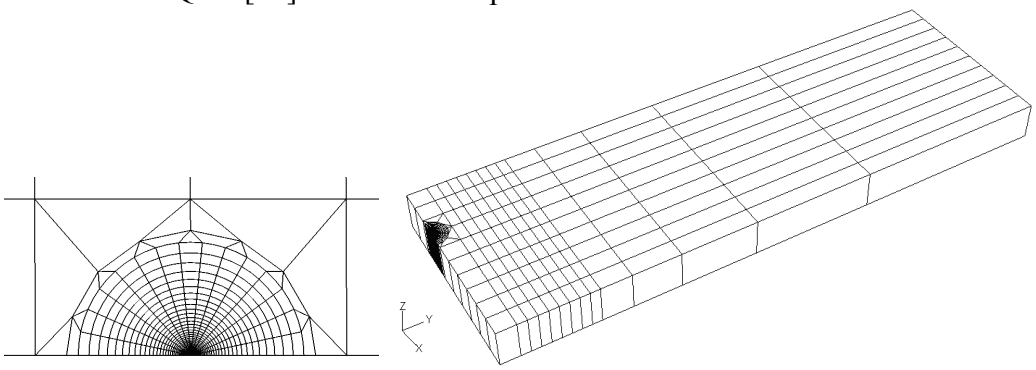

Figure 2. Typical FEA mesh, $a/W = 0.3$

Based on some stress component with corresponding finite element solutions at one or several locations (points) within the plastic zone, Yang *et al*. [9, 10] determine the A_2 values by matching a three-term expansion on crack-tip stress field. It is called the "*point match*" method by some researchers. Also based on FEA results, Nikishkov *et al*. [12] suggest a "*fitting method*" to determine parameter A values through a three-term expansion expressed by Eq. (2). In the present work, the proposed least square fitting method is utilized to obtained numerical solutions of constraint parameter A. See refs. [12] and [13] for more details about the procedure of the fitting method.

3. Finite element analysis, results and discussion

3.1. Material model and properties

The material model for finite element analyses carried out in the present work is the deformation theory of plasticity. Ramberg-Osgood power-law strain hardening relation is applied in finite element code ABAQUS [18], which is used in the present FEA.

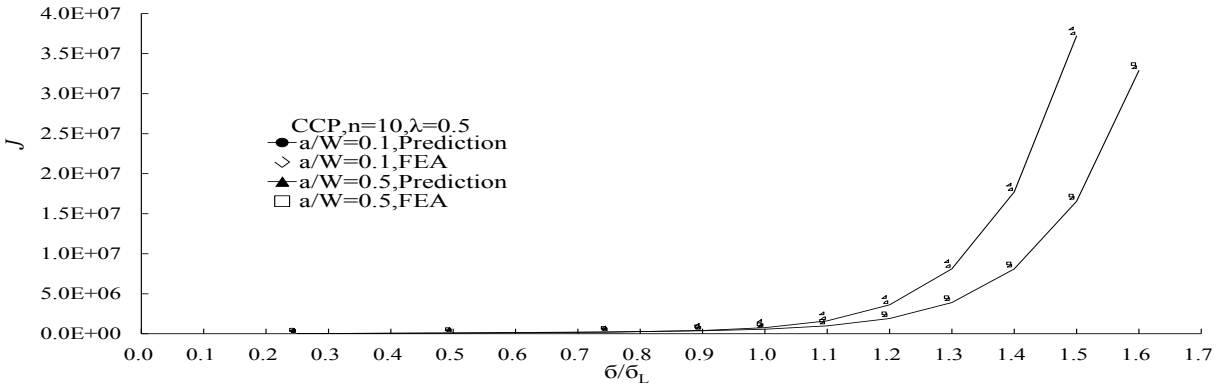

Figure 3. Comparisons of *J*-integral, CCP

Material properties used for all the analyses are specified as follows, yield stress $\sigma_0=4.0\times10^8$ *Pa*, elasticity modulus $E=2.0\times10^{11}$ *Pa*, Poisson ratio $\upsilon=0.3$, material coefficient $\alpha=1.0$, and hardening exponent n=3, 4, 5, 7 and 10. The used material properties cover a wide range of both high and low strain hardening behaviors.

3.2. 2D cracked models and FEA procedure

Three typical cracked specimens under biaxial loading (shown in Figure 1), *i.e.* single edge cracked plate (SECP), center cracked plate (CCP) and double edge cracked plate (DECP), are studied through finite element analysis method. Due to the symmetry of the specimens, only a half of the SECP or a quarter of the CCP or DECP structure is modeled in the finite element analyses. A typical three-dimensional (3D) finite element mesh used for all three specimen models is illustrated in Figure 2. Total 1196 elements are included in the mesh and element type is assigned as 20-node quadratic hybrid brick with linear pressure, reduced integration [18]. Element radial sizes of finite element mesh are varied according to a geometric progression. The value for geometry size ratio of height over width, *H/W*, is 3.0. This 3D mesh is utilized to simulate 2D plane strain conditions with an additional boundary condition, the displacement in the model thickness direction $u_z=0$. Finite element analyses for all three specimens (SECP, CCP and DECP) are carried out with two values of biaxial loading ratio, $\lambda=\sigma_x/\sigma_y=0.5$, and 1.0 (see Figure 1). The external loads applied on the remote end of the specimens are normalized by yield stress σ_0, *i.e.* σ/σ_0.

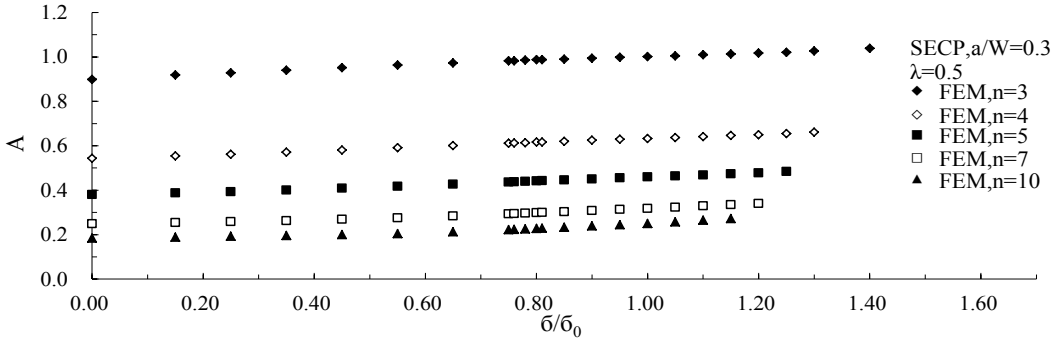

Figure 4. FEA solutions of constraint parameter *A* for SECP, *a/W*=0.3, λ=0.5

The fitting area to calculate the values of parameter *A* from FEA results by a least square fitting method suggested by Nikishkov *et al*. (see [12, 14]) is set as $1.5 \le \bar{r} \le 3$ and $0^0 \le \theta \le 45^0$, and the opening stress, σ_θ, is set as the stress component used for the least square fitting process.

Verifications of the used finite element model (mesh) and succedent fitting process for *A* values determination are carried out through comparison of solutions for two fracture parameters, load-related parameter *J*-integral and constraint parameter *Q* (*J*-*Q* approach). The comparison is based on *J*-integral estimation formulas and solutions of parameter *Q* for CCP specimen under

biaxial loading reported in the literature.

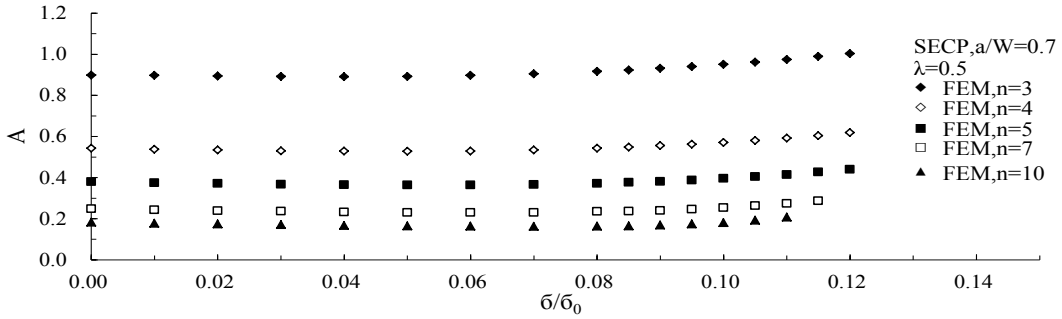

Figure 5. . FEA solutions of constraint parameter A for SECP, a/W=0.7, λ=0.5

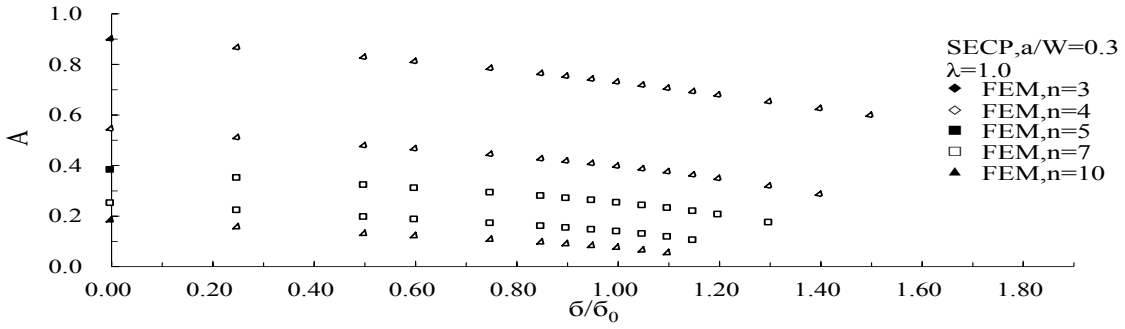

Figure 6. . FEA solutions of constraint parameter A for SECP, a/W=0.3, λ=1.0

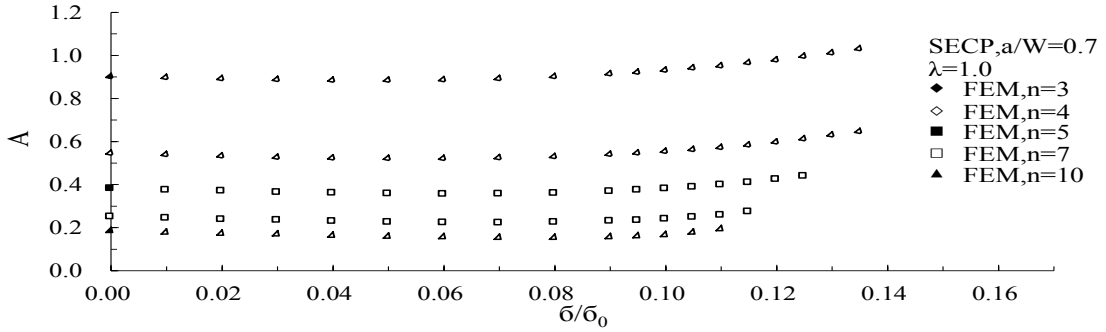

Figure 7. . FEA solutions of constraint parameter A for SECP, a/W=0.7, λ=1.0

For the purpose of comparison, finite element analysis for CCP specimen is carried out with hardening exponent n=10 for biaxial loading ratio λ=0.5 and geometry ratio a/W=0.1, 0.5. The values for J-integral from finite element analysis are compared with those obtained from EPRI estimation formulas of J [19]. Figure 3 shows the comparison results for a/W=0.1 and 0.5. It can be found that the J-integral values from FEA are very close to those from the estimation formulas. Based on the results of finite element analysis, constraint parameter A can also be obtained by using the fitting method proposed by Nikishkov *et al*. [12]. Through relationship between A and Q presented in authors' previous paper [13], the obtained solutions for A are converted to values of Q. Then determined Q values are compared with those reported by O'Dowd *et al.* [19]. It is found that, for both relative crack length a/W=0.1 and 0.5, Q solutions from the preset FEA results are close to those obtained by O'Dowd *et al.* [19]. As a numerical example, data comparison between Q values from FEA as well as A-Q relationship and those presented by O'Dowd *et al* [19] for the CCP under n=10 with a/W=0.5 and λ=0.5 is shown in Table 1.

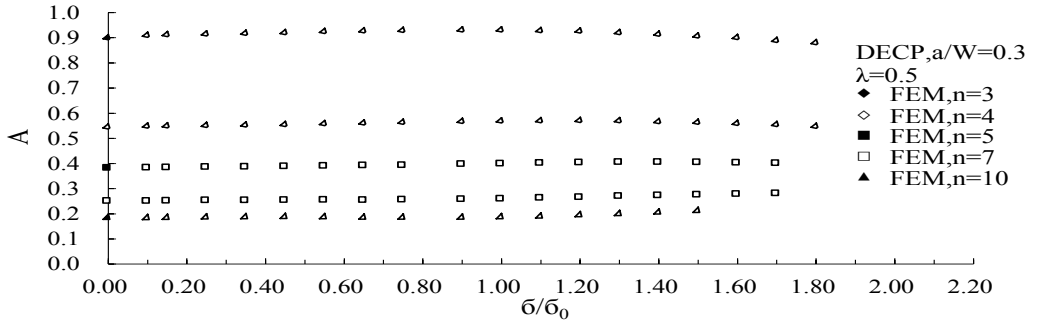

Figure 8. . FEA solutions of constraint parameter *A* for DECP, *a/W*=0.3, λ=0.5

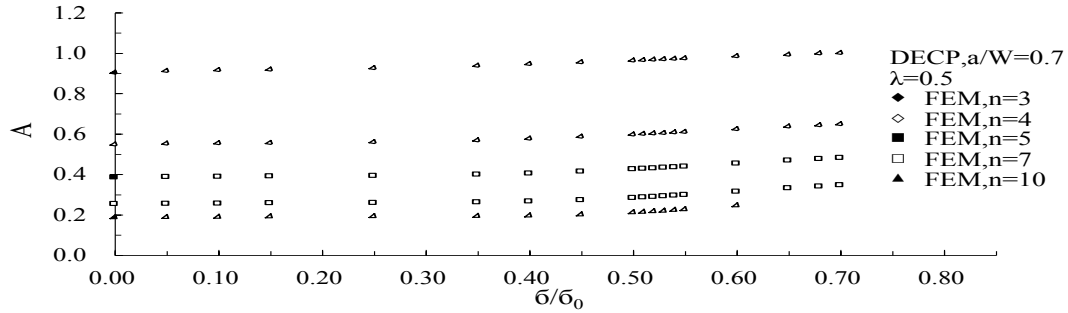

Figure 9. . FEA solutions of constraint parameter *A* for DECP, *a/W*=0.7, λ=0.5

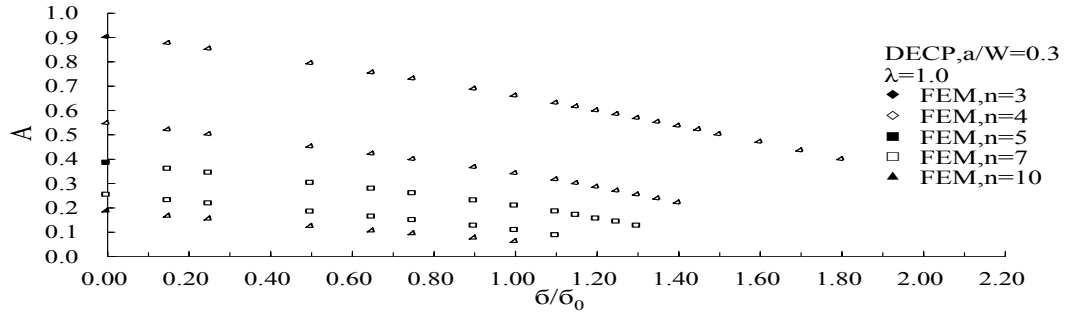

Figure 10. . FEA solutions of constraint parameter *A* for DECP, *a/W*=0.3, λ=1.0

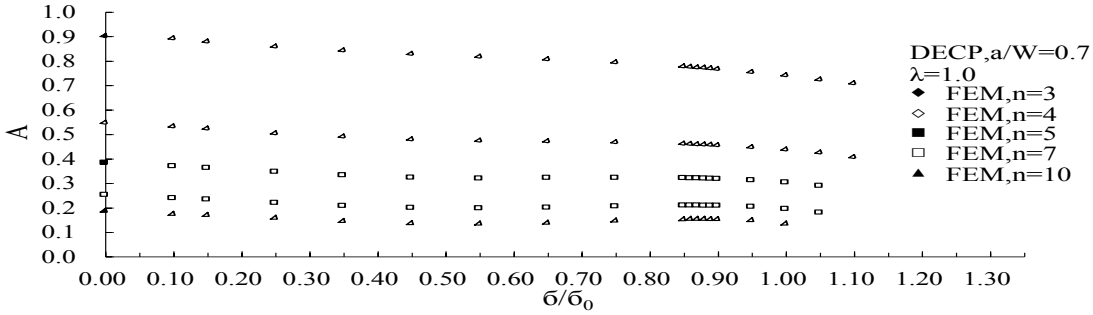

Figure 11. . FEA solutions of constraint parameter *A* for DECP, *a/W*=0.7, λ=1.0

3.3. FEA results

In the present work, a wide range of finite element analyses for three typical specimens (SECP, CCP and DECP) under biaxial loading are completed. Based on the FEA results, numerical solutions of constraint parameter *A* are determined by using the fitting method suggested by Nikishkov *et al*. [12].

The research of Chao and Zhu [20] on 2D plane strain models shows that the size requirement for ductile fracture initiation under J-A_2 dominant conditions is $a\sigma_0/J > 6$ for the shallow cracked cases or $b\sigma_0/J > 11$ for deep cracked cases, where a is the crack length and b is the remaining ligament. In the present finite element analyses (FEA), the highest load levels are those corresponding to the values mentioned above. In addition, Chao and Zhu [20] also argue that, for deep crack cases, a value of $b\sigma_0/J$ around 30 corresponds to fully plastic condition, while for shallow cracks, values of $a\sigma_0/J \leq 50$ already nearly correspond to the fully plastic deformation.

Table 2. FEA results for SECP specimen under λ=0.5

a/W	0.1						0.3				
σ/σ_0	n=3	n=4	n=5	n=7	n=10	σ/σ_0	n=3	n=4	n=5	n=7	n=10
0.250	0.91524	0.55153	0.38552	0.25194	0.18600	0.150	0.91848	0.55422	0.38785	0.25432	0.18828
0.500	0.92583	0.55861	0.39022	0.25514	0.18820	0.250	0.92787	0.56120	0.39339	0.25847	0.19307
0.750	0.93635	0.56870	0.39808	0.25894	0.18998	0.350	0.93984	0.57046	0.40079	0.26298	0.19567
0.900	0.93816	0.57312	0.40230	0.26189	0.19169	0.450	0.95082	0.58010	0.40830	0.26851	0.19989
1.000	0.93815	0.57465	0.40464	0.26473	0.19350	0.550	0.96266	0.59058	0.41728	0.27570	0.20481
1.100	0.93624	0.57543	0.40646	0.26701	0.19586	0.650	0.97216	0.60094	0.42667	0.28420	0.21255
1.200	0.93422	0.57461	0.40738	0.26909	0.19841	0.750	0.98224	0.61135	0.43656	0.29347	0.22260
1.300	0.92749	0.57367	0.40708	0.27057	0.20102	0.760	0.98243	0.61224	0.43751	0.29452	0.22376
1.400	0.92144	0.57114	0.40649	0.27139	0.20346	0.780	0.98498	0.61374	0.43951	0.29626	0.22521
1.450	0.91770	0.56776	0.40569	0.27165	0.20471	0.800	0.98738	0.61595	0.44135	0.29836	0.22766
1.500	0.91686	0.56569	0.40371	0.27184	0.20520	0.810	0.98750	0.61664	0.44223	0.29939	0.22884
1.600	0.90796	0.56079	0.40124	0.27086	0.20712	0.850	0.98972	0.62004	0.44594	0.30331	0.23291
1.700	0.89741	0.55511	0.39682	0.26981	0.20857	0.900	0.99387	0.62480	0.45027	0.30814	0.23877
1.800	0.89022	0.54923	0.39370	0.26909	0.21073	0.950	0.99752	0.62919	0.45497	0.31297	0.24481
1.900	0.88251	0.54524	0.39123	0.26969		1.000	1.00097	0.63260	0.45915	0.31797	0.25032
2.000	0.87144	0.54097	0.39000	0.27253		1.050	1.00410	0.63700	0.46394	0.32345	0.25702
2.100	0.86730	0.53830	0.39109			1.100	1.00960	0.64135	0.46831	0.32895	0.26489
2.200	0.85850	0.53831	0.39465			1.150	1.01256	0.64566	0.47320	0.33449	0.27227
2.300	0.85574	0.53960	0.40008			1.200	1.01744	0.64968	0.47739	0.34043	
2.400	0.85089	0.54220	0.40819			1.250	1.02045	0.65409	0.48381		
2.500	0.84605	0.54595	0.40777			1.300	1.02606	0.66051			
						1.400	1.03790				
a/W	0.5						0.7				
σ/σ_0	n=3	n=4	n=5	n=7	n=10	σ/σ_0	n=3	n=4	n=5	n=7	n=10
0.050	0.90776	0.54631	0.38146	0.24915	0.18447	0.010	0.89720	0.53809	0.37467	0.24350	0.17829
0.100	0.91152	0.54799	0.38246	0.25035	0.18470	0.020	0.89423	0.53474	0.37177	0.23876	0.17434
0.150	0.91955	0.55268	0.38576	0.25173	0.18561	0.030	0.89173	0.53033	0.36724	0.23706	0.17199
0.200	0.93053	0.56034	0.39127	0.25422	0.18691	0.040	0.89061	0.52866	0.36531	0.23293	0.16760
0.250	0.94523	0.57130	0.39853	0.25971	0.18961	0.050	0.89235	0.52783	0.36371	0.23065	0.16503
0.290	0.95976	0.58280	0.40750	0.26493	0.19437	0.060	0.89697	0.52928	0.36403	0.22991	0.16382
0.320	0.97212	0.59245	0.41527	0.27163	0.20003	0.070	0.90474	0.53483	0.36613	0.23019	0.16289
0.350	0.98591	0.60372	0.42555	0.28017	0.20751	0.080	0.91638	0.54304	0.37198	0.23524	0.16446
0.380	1.00133	0.61660	0.43649	0.29048	0.21678	0.085	0.92330	0.54792	0.37719	0.23715	0.16544
0.400	1.01265	0.62591	0.44562	0.29848	0.22604	0.090	0.93138	0.55575	0.38172	0.24035	0.16915
0.420	1.02430	0.63620	0.45449	0.30771	0.23951	0.095	0.94057	0.56281	0.38760	0.24638	0.17440
0.440	1.03745	0.64737	0.46606	0.32072		0.100	0.95116	0.57116	0.39635	0.25400	0.18140
0.450	1.04403	0.65423	0.47252	0.32716		0.105	0.96122	0.58068	0.40441	0.26322	0.19312
0.460	1.05195	0.66160	0.47764	0.33425		0.110	0.97422	0.59175	0.41412	0.27427	0.20781
0.470	1.05901	0.66752	0.48483	0.34231		0.115	0.98931	0.60421	0.42753	0.28745	
0.480	1.06637	0.67394	0.49279			0.120	1.00308	0.61856	0.44058		
0.490	1.07404	0.68244	0.50135								
0.500	1.08353	0.69169	0.50789								
0.510	1.09180	0.69890	0.51741								

According to the above criteria, the external load ratios (σ/σ_0) used here to determine numerical solutions for parameter A from FEA for the three specimens cover the deformation range from small-scale yielding (SSY) to large-scale yielding (LSY). For example, for SECP with a/W=0.7

(deep crack), the values of $b\sigma_0/J$ at maximum loads are within 54-64 and 38-62 for λ=0.5 and λ=1.0, respectively. For the SECP with a/W=0.3 (shallow crack), the values of $a\sigma_0/J$ at maximum loads are around 4 and within 4-8 for λ=0.5 and 1.0, respectively.

Table 3. FEA results for SECP specimen under λ=1.0

a/W	0.1					0.3					
σ/σ_0	n=3	n=4	n=5	n=7	n=10	σ/σ_0	n=3	n=4	n=5	n=7	n=10
0.100	0.87886	0.52283	0.36139	0.23252	0.16637	0.250	0.86428	0.50841	0.34846	0.22094	0.15636
0.150	0.87193	0.51733	0.35721	0.22864	0.16388	0.500	0.82627	0.47641	0.32046	0.19371	0.12998
0.200	0.86218	0.50929	0.35109	0.22374	0.16031	0.600	0.80984	0.46398	0.30834	0.18463	0.12093
0.250	0.85161	0.49880	0.34068	0.21418	0.15242	0.750	0.78229	0.44228	0.29016	0.16935	0.10651
0.350	0.82909	0.47963	0.32432	0.20187	0.13979	0.850	0.76195	0.42490	0.27680	0.15829	0.09611
0.500	0.79407	0.45111	0.30062	0.18177	0.12125	0.900	0.75108	0.41559	0.26863	0.15116	0.08927
0.600	0.77063	0.43254	0.28539	0.16720	0.10688	0.950	0.73967	0.40585	0.25995	0.14343	0.08173
0.750	0.73304	0.40275	0.25903	0.14895	0.09111	1.000	0.72792	0.39549	0.25051	0.13646	0.07483
0.850	0.70541	0.37904	0.24150	0.13336	0.08086	1.050	0.71585	0.38461	0.24033	0.12657	0.06438
0.900	0.69224	0.36832	0.23012	0.12645	0.07315	1.100	0.70320	0.37306	0.22917	0.11525	0.05330
0.950	0.67725	0.35462	0.22064	0.11689	0.06747	1.150	0.69053	0.36099	0.21703	0.10185	
1.000	0.66360	0.34334	0.20847	0.10631	0.05870	1.200	0.67721	0.34673	0.20361		
1.050	0.64850	0.32933	0.19825	0.09724		1.300	0.65063	0.31715	0.17182		
1.100	0.63293	0.31458	0.18450	0.08444		1.400	0.62324	0.28424			
1.150	0.61916	0.30239	0.16985	0.06920		1.500	0.59711				
1.200	0.60332	0.28683	0.15454								
1.250	0.58730	0.27077	0.13766								
1.300	0.57114	0.25416									
1.400	0.53570	0.21928									
1.500	0.50197	0.18206									
1.600	0.46465										
a/W	0.5					0.7					
σ/σ_0	n=3	n=4	n=5	n=7	n=10	σ/σ_0	n=3	n=4	n=5	n=7	n=10
0.050	0.89539	0.53593	0.37253	0.24163	0.17648	0.010	0.89473	0.53599	0.37287	0.24197	0.17685
0.100	0.88733	0.52721	0.36488	0.23443	0.17060	0.020	0.88944	0.53067	0.36825	0.23572	0.17150
0.150	0.88333	0.52205	0.35942	0.22926	0.16424	0.030	0.88477	0.52430	0.36202	0.23258	0.16777
0.200	0.88231	0.51950	0.35476	0.22375	0.15827	0.040	0.88147	0.52076	0.35844	0.22695	0.16194
0.250	0.88454	0.52020	0.35377	0.21954	0.15259	0.050	0.88117	0.51803	0.35517	0.22317	0.15793
0.300	0.89055	0.52282	0.35431	0.21939	0.14867	0.060	0.88350	0.51901	0.35378	0.22090	0.15523
0.350	0.89971	0.52851	0.35893	0.22101	0.14978	0.070	0.88898	0.52136	0.35405	0.21952	0.15264
0.380	0.90671	0.53415	0.36306	0.22482	0.15137	0.080	0.89831	0.52735	0.35806	0.22293	0.15239
0.400	0.91272	0.54037	0.36806	0.22831	0.15571	0.090	0.91089	0.53800	0.36607	0.22799	0.15500
0.420	0.91989	0.54386	0.37220	0.23301	0.16182	0.095	0.91888	0.54394	0.37266	0.23134	0.15918
0.440	0.92651	0.55243	0.37959	0.23953		0.100	0.92830	0.55118	0.37852	0.23782	0.16529
0.450	0.93211	0.55492	0.38148	0.24372		0.105	0.93908	0.55960	0.38576	0.24612	0.17609
0.460	0.93605	0.56045	0.38644	0.24899		0.110	0.94889	0.56956	0.39663	0.25629	0.19288
0.470	0.94035	0.56369	0.39208	0.25838		0.115	0.96294	0.58105	0.40683	0.27180	
0.480	0.94748	0.57034	0.39848	0.26546		0.120	0.97548	0.59448	0.42219		
0.490	0.95240	0.57420	0.40189			0.125	0.99333	0.60988	0.43656		
0.500	0.95775	0.57854	0.40964			0.130	1.00926	0.62795			
						0.135	1.02745	0.64357			

The obtained numerical solutions of A for biaxial loading ratios λ=0.5 and 1.0 and relative crack lengths a/W=0.1, 0.3, 0.5, 0.7 are listed in Tables 2-3, 4-5 and 6-7 for the SECP, CCP and DECP specimens, respectively. Typical numerical solutions for parameter A for a/W=0.3, 0.7 are presented in Figures 4-5 (λ=0.5) and Figures 6-7 (λ=1.0) for the SECP specimen as well as Figures 8-9 (λ=0.5) and Figures 10-11 (λ=1.0) for DECP specimen.

3.4. Discussions on FEA results and constraint effect

Examining the solutions of A obtained from FEA results for the SECP, CCP and DECP specimens under biaxial loading, it is found that, the curve shape similarity observed by Nikishkov *et al*. [12]

not only appear in the cases of uniaxial loading and external loading ratio σ/σ_L (σ_L, limit load of specimen) but also in the cases of biaxial loading and loading normalization, σ/σ_0, see Figure 4-7 for example.

Table 4. FEA results for CCP specimen under λ=0.5

a/W	0.1						0.3				
σ/σ_0	n=3	n=4	n=5	n=7	n=10	σ/σ_0	n=3	n=4	n=5	n=7	n=10
0.500	1.03293	0.64948	0.46887	0.32352	0.25390	0.250	0.98134	0.60644	0.43267	0.29277	0.22469
0.700	1.07906	0.68806	0.50129	0.34936	0.27751	0.500	1.05796	0.66917	0.48450	0.33539	0.26464
0.900	1.11904	0.71974	0.52744	0.36991	0.29557	0.750	1.12909	0.73037	0.53563	0.37581	0.30014
1.000	1.13527	0.73370	0.53894	0.37836	0.30237	0.900	1.16595	0.76170	0.56335	0.39798	0.31924
1.200	1.15529	0.75361	0.55608	0.39210	0.31170	1.000	1.18836	0.77990	0.58012	0.41203	0.33108
1.500	1.16895	0.76686	0.56621	0.39975	0.31748	1.100	1.20084	0.79773	0.59419	0.42491	0.34168
1.800	1.16139	0.75712	0.56246	0.39239	0.31165	1.200	1.21286	0.80829	0.60522	0.43449	0.35199
2.000	1.13246	0.74272	0.54581	0.38135	0.30277	1.300	1.22667	0.81872	0.61313	0.44234	0.36159
2.100	1.11699	0.73432	0.53681	0.37501	0.29808	1.400	1.22663	0.82549	0.62225	0.44924	0.37116
2.200	1.09825	0.71748	0.52619	0.36777	0.29321	1.450	1.22873	0.82394	0.62381	0.45351	0.37509
2.300	1.08745	0.70466	0.51373	0.35901	0.28309	1.500	1.22943	0.82773	0.62419	0.45429	0.37893
2.400	1.06267	0.68221	0.49896	0.34764	0.27633	1.550	1.22865	0.83059	0.62359	0.45407	0.37497
2.450	1.04035	0.67860	0.49075	0.34698		1.600	1.22625	0.82498	0.62134	0.45371	0.38314
2.500	1.03254	0.66464	0.48187	0.33447		1.650	1.22214	0.82517	0.62323	0.45807	0.39281
2.600	1.01409	0.64474	0.46421			1.700	1.21616	0.82321	0.62016	0.44720	0.39826
2.700	0.97462	0.62172				1.750	1.20833	0.81313	0.61771	0.46113	0.40449
						1.800	1.21234	0.81012	0.59436	0.45637	0.41530
a/W	0.5						0.7				
σ/σ_0	n=3	n=4	n=5	n=7	n=10	σ/σ_0	n=3	n=4	n=5	n=7	n=10
0.100	0.94657	0.57838	0.40893	0.27252	0.20548	0.050	0.94003	0.57410	0.40565	0.27004	0.20336
0.150	0.96767	0.59526	0.42335	0.28498	0.21745	0.100	0.97886	0.60394	0.43006	0.28991	0.22255
0.250	1.01066	0.63010	0.45229	0.30762	0.23933	0.150	1.01980	0.63643	0.45724	0.31137	0.24264
0.350	1.05770	0.66699	0.48260	0.33321	0.26171	0.250	1.11106	0.71061	0.51835	0.36082	0.28602
0.450	1.10582	0.70680	0.51559	0.35931	0.28520	0.350	1.19965	0.79269	0.59128	0.42146	0.34039
0.550	1.15103	0.74722	0.55041	0.38757	0.31005	0.400	1.24116	0.83100	0.62637	0.45712	0.37568
0.650	1.19119	0.78594	0.58557	0.41778	0.33689	0.450	1.28136	0.86873	0.66098	0.49110	0.41489
0.750	1.23122	0.82265	0.61827	0.44734	0.36587	0.460	1.28455	0.87745	0.66976	0.49773	0.42362
0.850	1.25716	0.85287	0.64612	0.47604	0.39809	0.470	1.29303	0.88141	0.67470	0.50429	0.43117
0.900	1.27272	0.86516	0.65953	0.48757	0.41343	0.480	1.30103	0.89001	0.68317	0.51077	0.43860
0.950	1.28575	0.87540	0.66842	0.49850	0.42643	0.490	1.30828	0.89773	0.68769	0.51719	0.44600
1.000	1.29677	0.88340	0.67961	0.50783	0.44074	0.500	1.31593	0.90135	0.69194	0.52353	0.45333
1.050	1.30484	0.89560	0.68895	0.51551	0.45175	0.510	1.31719	0.90949	0.70028	0.52982	0.45925
1.100	1.31050	0.89834	0.69041	0.51172	0.46758	0.550	1.34438	0.93362	0.72286	0.55120	0.48569
1.150	1.31258	0.90536	0.69556	0.53219	0.48279	0.580	1.36147	0.94855	0.73659	0.56478	0.50540
1.200	1.32147	0.90225	0.70169	0.54275		0.600	1.37217	0.95601	0.74623	0.57506	0.50833
						0.620	1.37384	0.96127	0.75475	0.58194	
						0.640	1.38217	0.97261	0.75650	0.57980	
						0.660	1.39806	0.98232	0.76824	0.59876	

By analyzing the numerical solutions of parameter *A* for three cracked specimens (see Tables 2-7, Figures 4-11), several dependencies have been found. First, it is found that, for any specific specimen geometry (*a/W*) of some cracked body (SECP, CCP or DECP), generally the maximum external loading ratios (σ/σ_0), which are determined by the criteria suggested by Chao and Zhu [20], increase with decreasing of hardening coefficient *n*.

In addition, the effects of crack geometry, hardening exponent (*n*) and biaxial loading ratio (λ) on parameter *A* (constraint level) are also observed. For uniaxial loading cases (λ=0.0) investigated in a previous work of authors [13], it has been shown that *A* values gradually increase with external loading. The results in the current work show that, with smaller biaxial loading ratio (λ=0.5), the parameter *A* follows a general decreasing trend with increasing external loading for shallow crack geometries (*e.g.* *a/W*=0.1 for SECP and CCP, *a/W*=0.1, 0.3 for DECP). Decreased values for parameter *A* indicate the increasing constraint level. For the cases with bigger biaxial loading ratio (λ=1.0), a decreasing trend of parameter *A* appears not only for those shallowest cracks but also for cracks with larger depth and even fairly deep cracks (*e.g.* *a/W*=0.3 for SECP, 0.3, 0.5 for CCP, 0.5,

0.7 for DECP). On the other hand, generally, a deep crack is not sensitive to the variation of the λ value, except in the case of DECP. For example, for SECP, with λ value increasing from 0.5 to 1.0, the trend of *A* curves for *a/W*=0.3 (shallow crack) changes from increasing to decreasing (see Figure 4 and Figure 6), while that for *a/W*=0.7 (deep crack) almost keeps no change (see Figure 5 and Figure 7).

Table 5. FEA results for CCP specimen under λ=1.0

a/W	0.1					0.3					
σ/σ_0	n=3	n=4	n=5	n=7	n=10	σ/σ_0	n=3	n=4	n=5	n=7	n=10
0.500	0.89279	0.53665	0.37503	0.24536	0.18130	0.500	0.91158	0.55164	0.38764	0.25670	0.19110
0.750	0.87398	0.52211	0.36309	0.23732	0.17650	0.750	0.90119	0.54687	0.38453	0.25403	0.19075
0.900	0.85974	0.51059	0.35378	0.23024	0.17073	0.900	0.89260	0.53934	0.37876	0.25124	0.18810
1.000	0.84974	0.50165	0.34734	0.22645	0.16867	1.000	0.88388	0.53271	0.37344	0.24757	0.18544
1.200	0.82588	0.48414	0.33109	0.21159	0.15611	1.200	0.86152	0.51500	0.35847	0.23465	0.17641
1.400	0.79886	0.46125	0.31191	0.19430	0.13836	1.300	0.84798	0.50381	0.34851	0.22595	0.16850
1.500	0.78414	0.44974	0.30024	0.18333	0.12928	1.400	0.83435	0.49110	0.33705	0.21513	0.15796
1.700	0.75316	0.42327	0.27812	0.16285	0.10628	1.500	0.81667	0.47705	0.32418	0.20261	0.14473
1.900	0.71719	0.39497	0.25383	0.14332	0.08701	1.600	0.79928	0.46145	0.30956	0.18870	0.12943
2.100	0.67310	0.36392	0.22880	0.12295	0.07116	1.700	0.77977	0.44471	0.29429	0.17382	
2.250	0.63545	0.33786	0.20833	0.10738	0.06048	1.800	0.75775	0.42657	0.27752	0.15722	
2.300	0.62310	0.32864	0.20185	0.10326	0.05819	1.900	0.73375	0.40695	0.25987		
2.400	0.59669	0.30860	0.18622	0.09313		2.000	0.70638	0.38399	0.24039		
2.500	0.56789	0.28749	0.17001	0.08243		2.100	0.67493	0.36126			
						2.200	0.64552				
a/W	0.5					0.7					
σ/σ_0	n=3	n=4	n=5	n=7	n=10	σ/σ_0	n=3	n=4	n=5	n=7	n=10
0.150	0.92731	0.56293	0.39591	0.26173	0.19560	0.020	0.91750	0.55434	0.38870	0.25562	0.19002
0.250	0.94008	0.57296	0.40354	0.26788	0.20128	0.050	0.92701	0.56345	0.39655	0.26195	0.19615
0.350	0.95237	0.58435	0.41347	0.27599	0.20909	0.080	0.94209	0.57458	0.40569	0.26987	0.20313
0.450	0.96587	0.59477	0.42278	0.28397	0.21564	0.100	0.95152	0.58162	0.41110	0.27409	0.20682
0.550	0.97609	0.60460	0.43141	0.29068	0.22245	0.120	0.96133	0.58941	0.41727	0.27917	0.21165
0.650	0.98365	0.61287	0.43900	0.29739	0.22770	0.150	0.97688	0.60129	0.42727	0.28709	0.21988
0.750	0.98812	0.61906	0.44531	0.30295	0.23276	0.180	0.99285	0.61442	0.43815	0.29533	0.22757
0.800	0.98985	0.62150	0.44737	0.30518	0.23472	0.200	1.00380	0.62312	0.44522	0.30168	0.23244
0.850	0.99025	0.62319	0.44922	0.30709	0.23698	0.220	1.01481	0.63209	0.45263	0.30755	0.23784
0.900	0.98949	0.62396	0.45041	0.30859	0.23838	0.250	1.03259	0.64629	0.46423	0.31652	0.24565
0.920	0.98942	0.62418	0.45089	0.30906	0.23877	0.270	1.04286	0.65555	0.47222	0.32281	0.25105
0.930	0.98763	0.62363	0.45059	0.30919	0.23914	0.280	1.04963	0.66082	0.47647	0.32620	0.25416
0.940	0.98931	0.62443	0.45123	0.30928	0.23916	0.290	1.05454	0.66546	0.48050	0.32960	0.25676
0.950	0.98723	0.62383	0.45089	0.30952	0.23905	0.300	1.06127	0.67082	0.48454	0.33284	0.25996
1.100	0.98060	0.61937	0.44883	0.30853	0.24025	0.350	1.08686	0.69490	0.50622	0.35042	0.27532
1.200	0.96946	0.61318	0.44308	0.30531	0.23882	0.400	1.11401	0.72094	0.52818	0.36947	0.29217
1.300	0.95729	0.60259	0.43585	0.29999	0.23579	0.450	1.13808	0.74526	0.55133	0.38980	0.31163
1.400	0.93431	0.58766	0.42178	0.28988	0.23386	0.500	1.15667	0.76722	0.57125	0.41117	0.33520
1.450	0.92294	0.57975	0.41574	0.28653	0.22748	0.540	1.17207	0.78207	0.58696	0.42791	0.35614
1.500	0.90961	0.56595	0.40578	0.28015	0.22326	0.570	1.18153	0.79379	0.59996	0.44119	0.37169
1.550	0.89519	0.55579	0.39827	0.27265		0.600	1.18951	0.80087	0.60980	0.45302	0.38818
1.600	0.88749	0.54476	0.39138	0.25768		0.620	1.19964	0.80759	0.61426	0.45920	0.40008
1.650	0.87294					0.650	1.20579	0.81690	0.62560	0.47051	0.41449
						0.700	1.21008	0.82964	0.63574	0.48499	
						0.750	1.21750	0.83818	0.64569	0.49148	

As for the effect of hardening exponent (*n*), with the increase of the biaxial loading ratio λ, decreasing trend of *A* curves appears earlier (under smaller external loading) or is more significant for cases with smaller *n* values than that for cases with bigger *n* values. For example, for DECP, the trend of the *A* curves for *a/W*=0.3 changes from increasing to decreasing as λ increases from 0.5 to 1.0 (see Figures 8 and 10 as well as Tables 6 and 7), but the curve for *n*=3 decreases more quickly than that for *n*=10 (see Figures 10 and Table 7).

Table 6. FEA results for DECP specimens under λ=0.5

a/W	0.1					0.3					
σ/σ_0	n=3	n=4	n=5	n=7	n=10	σ/σ_0	n=3	n=4	n=5	n=7	n=10
0.150	0.90737	0.54685	0.38224	0.24968	0.18406	0.100	0.90818	0.54679	0.38187	0.24907	0.18328
0.250	0.91158	0.54958	0.38434	0.24954	0.18362	0.150	0.91077	0.54809	0.38272	0.24964	0.18426
0.450	0.91661	0.55176	0.38502	0.25097	0.18526	0.250	0.91332	0.54994	0.38431	0.25151	0.18576
0.650	0.92183	0.55453	0.38650	0.25036	0.18286	0.350	0.91581	0.55120	0.38497	0.25171	0.18676
0.800	0.92350	0.55846	0.38904	0.25207	0.18261	0.450	0.91898	0.55328	0.38644	0.25232	0.18717
0.900	0.92404	0.55951	0.39042	0.25231	0.18207	0.550	0.92276	0.55630	0.38841	0.25332	0.18683
1.000	0.92281	0.55986	0.39114	0.25285	0.18237	0.650	0.92587	0.55910	0.38993	0.25278	0.18533
1.100	0.91969	0.55978	0.39137	0.25287	0.18183	0.750	0.92773	0.56158	0.39163	0.25428	0.18495
1.200	0.91664	0.55808	0.39106	0.25291	0.18259	0.900	0.92889	0.56526	0.39526	0.25590	0.18511
1.300	0.91133	0.55569	0.39007	0.25310	0.18236	1.000	0.92894	0.56735	0.39783	0.25800	0.18644
1.400	0.90467	0.55211	0.38811	0.25245	0.18210	1.100	0.92694	0.56796	0.40010	0.26100	0.18924
1.500	0.89569	0.54713	0.38449	0.25125	0.18167	1.200	0.92502	0.56908	0.40195	0.26447	0.19433
1.600	0.88816	0.54103	0.38036	0.24910	0.18155	1.300	0.91854	0.56778	0.40363	0.26817	0.19935
1.700	0.87634	0.53350	0.37532	0.24657	0.18074	1.400	0.91268	0.56469	0.40386	0.27134	0.20534
1.800	0.86651	0.52693	0.37039	0.24319	0.17890	1.500	0.90479	0.56190	0.40302	0.27421	0.21158
1.900	0.85595	0.51778	0.36420	0.23931	0.17728	1.600	0.89916	0.55791	0.40105	0.27645	
2.000	0.84454	0.51006	0.35776	0.23568	0.17673	1.700	0.88761	0.55272	0.39962	0.27887	
2.100	0.83298	0.50128	0.35187	0.23310		1.800	0.87853	0.54614	0.39536		
2.200	0.82121	0.49443	0.34718	0.23264		1.900	0.86295	0.53798	0.39186		
2.300	0.81263	0.48848	0.34429			2.000	0.85140	0.53106			
2.400	0.80199	0.48358	0.34293			2.100	0.84044	0.52425			
2.500	0.79129	0.47979									
2.600	0.78375	0.47724									
a/W	0.5					0.7					
σ/σ_0	n=3	n=4	n=5	n=7	n=10	σ/σ_0	n=3	n=4	n=5	n=7	n=10
0.150	0.91213	0.54967	0.38424	0.25152	0.18575	0.050	0.90756	0.54713	0.38246	0.24982	0.18460
0.250	0.91537	0.55176	0.38630	0.25296	0.18823	0.100	0.91131	0.54896	0.38365	0.25101	0.18524
0.350	0.92087	0.55515	0.38849	0.25473	0.18914	0.150	0.91350	0.55048	0.38552	0.25269	0.18811
0.450	0.92621	0.55914	0.39048	0.25557	0.18958	0.250	0.92076	0.55507	0.38757	0.25433	0.18911
0.550	0.93263	0.56450	0.39434	0.25664	0.18947	0.350	0.93280	0.56356	0.39414	0.25718	0.18980
0.650	0.93932	0.57156	0.40038	0.26070	0.19044	0.400	0.94105	0.57144	0.40002	0.26099	0.19214
0.750	0.94625	0.58013	0.40872	0.26762	0.19572	0.450	0.95005	0.58115	0.40893	0.26817	0.19751
0.800	0.94794	0.58492	0.41389	0.27244	0.20114	0.500	0.95887	0.59267	0.42054	0.27911	0.20770
0.850	0.95095	0.58934	0.41932	0.27876	0.20698	0.510	0.96088	0.59506	0.42304	0.28158	0.21009
0.900	0.95329	0.59420	0.42516	0.28572	0.21520	0.520	0.96283	0.59756	0.42566	0.28417	0.21276
0.920	0.95461	0.59628	0.42726	0.28844	0.21833	0.530	0.96481	0.60010	0.42834	0.28693	0.21570
0.940	0.95575	0.59727	0.42972	0.29143	0.22230	0.540	0.96671	0.60269	0.43112	0.29050	0.21966
0.950	0.95501	0.59886	0.43069	0.29296	0.22428	0.550	0.96864	0.60531	0.43396	0.29343	0.22287
1.050	0.95901	0.60715	0.44230	0.30817		0.600	0.97945	0.61862	0.44863	0.30978	0.24169
1.100	0.95830	0.61053	0.44644	0.31548		0.650	0.98736	0.63150	0.46353	0.32651	
1.150	0.95977	0.61315	0.45130	0.32235		0.680	0.99393	0.63871	0.47106	0.33586	
1.200	0.95740	0.61509	0.45563	0.32872		0.700	0.99604	0.64316	0.47639	0.34215	
1.250	0.95773	0.61597	0.45938	0.33408							

Based on the observations represented above, it can be concluded that, (1) in general, constraint level in crack-tip fields increases with the increase of biaxial loading ratio, λ; (2) the constraint level for materials with smaller values of hardening exponent *n* increases more with increased biaxial loading ratio; (3) the constraint level for shallow cracks rises more with increase of biaxial loading ratio; (4) comparing SECP and CCP specimens, an increase of biaxial loading ratio raises the constraint level of DECP more.

4. Conclusions

In this paper, numerical (finite element) solutions for the constraint parameter *A* for three plane strain mode I specimens, SECP, CCP and DECP, under biaxial load have been obtained based on the extensive finite element analyses of specimen crack-tip fields.

Table 7. FEA results for DECP specimens under λ=1.0

a/W	0.1						0.3				
σ/σ_0	n=3	n=4	n=5	n=7	n=10	σ/σ_0	n=3	n=4	n=5	n=7	n=10
0.150	0.86925	0.51533	0.35529	0.22685	0.16266	0.150	0.87254	0.51647	0.35567	0.22672	0.16228
0.250	0.84806	0.49772	0.34026	0.21168	0.14827	0.250	0.84930	0.49767	0.33986	0.21364	0.15104
0.500	0.78679	0.44669	0.29733	0.17643	0.11728	0.500	0.78991	0.44755	0.29760	0.17940	0.12105
0.650	0.74962	0.41600	0.27248	0.15509	0.09888	0.650	0.75172	0.41771	0.27370	0.15879	0.10214
0.750	0.72289	0.39416	0.25184	0.14370	0.08746	0.750	0.72614	0.39540	0.25541	0.14475	0.09047
0.900	0.68110	0.35892	0.22231	0.12096	0.06931	0.900	0.68443	0.36244	0.22572	0.12207	0.07298
1.000	0.65233	0.33357	0.20057	0.10054	0.05484	1.000	0.65589	0.33742	0.20404	0.10436	0.05877
1.100	0.62156	0.30469	0.17667	0.07855		1.100	0.62717	0.31193	0.18046	0.08248	
1.150	0.60835	0.29324	0.16211			1.150	0.61160	0.29698	0.16595		
1.200	0.59283	0.27797	0.14712			1.200	0.59593	0.28166	0.15098		
1.250	0.57732	0.26237	0.13066			1.250	0.58020	0.26597	0.13868		
1.300	0.56184	0.24644				1.300	0.56443	0.24989	0.12144		
1.350	0.54324	0.23021				1.350	0.54865	0.23344			
1.400	0.52774	0.21371				1.400	0.53291	0.21662			
1.450	0.51192	0.19698				1.450	0.51725				
1.500	0.49678					1.500	0.49766				
1.800	0.40071					1.600	0.46654				
1.900	0.36851					1.700	0.43085				
						1.800	0.39539				
a/W	0.5						0.7				
σ/σ_0	n=3	n=4	n=5	n=7	n=10	σ/σ_0	n=3	n=4	n=5	n=7	n=10
0.150	0.87424	0.51821	0.35734	0.22834	0.16451	0.100	0.88853	0.52789	0.36562	0.23577	0.17097
0.250	0.85134	0.49955	0.34149	0.21579	0.15266	0.150	0.87517	0.51917	0.35853	0.23019	0.16620
0.350	0.82888	0.48056	0.32587	0.20241	0.14183	0.250	0.85440	0.49999	0.34298	0.21630	0.15487
0.500	0.79558	0.45179	0.30169	0.18284	0.12336	0.350	0.83843	0.48690	0.32904	0.20342	0.14223
0.650	0.76040	0.42457	0.27963	0.16356	0.10690	0.450	0.82472	0.47563	0.31904	0.19605	0.13322
0.750	0.73700	0.40661	0.26290	0.15092	0.09652	0.550	0.81355	0.47025	0.31567	0.19398	0.13129
0.850	0.71251	0.38709	0.24703	0.13889	0.08753	0.650	0.80264	0.46755	0.31802	0.19668	0.13503
0.950	0.68765	0.36495	0.23096	0.12676	0.07590	0.750	0.79021	0.46407	0.31850	0.20183	0.14366
1.000	0.67356	0.35483	0.21976	0.12006	0.07036	0.850	0.77393	0.45752	0.31708	0.20500	0.14922
1.050	0.65937	0.34459	0.21074	0.10979		0.860	0.77172	0.45652	0.31663	0.20504	0.15020
1.100	0.64599	0.33115	0.20129	0.10092		0.870	0.76927	0.45543	0.31606	0.20495	0.15023
1.150	0.63102	0.32000	0.18807	0.09070		0.880	0.76820	0.45447	0.31541	0.20483	0.15019
1.200	0.61733	0.30549	0.17686	0.07515		0.890	0.76556	0.45323	0.31467	0.20457	0.15003
1.300	0.58549	0.27751	0.14798			0.900	0.76281	0.45187	0.31387	0.20437	0.15008
1.400	0.55166	0.24273				0.950	0.75103	0.44386	0.30871	0.19984	0.14562
1.500	0.51534	0.20277				1.000	0.73702	0.43410	0.29979	0.19153	0.13142
1.600	0.47414					1.050	0.72000	0.42111	0.28561	0.17653	
1.700	0.43161					1.100	0.70436	0.40281			

Through analyzing numerical solutions of constraint parameter *A*, several dependencies (mainly on the constraint effect) for 2D cracked models under biaxial loading are founded. They are:
(1) generally, the maximum external loading ratio (σ/σ_0) for which a valid solution can be obtained increases with decreasing hardening coefficient *n*;
(2) in general, the constraint level in crack-tip fields increases with an increase of biaxial loading ratio, λ;
(3) the constraint level for materials with smaller values of hardening exponent *n* rises more with increased biaxial loading ratio;
(4) the constraint level for shallow cracks increases more than for deep cracks with an increase of biaxial loading ratio;
(5) compared with SECP and CCP specimens, a higher biaxial loading ratio increases the constraint level of DECP more.
All numerical solutions for constraint parameter *A* under biaxial loading obtained in this work can be utilized to predict corresponding values for other two commonly-used constraint parameters A_2 and *Q* by the relationships between *A* and A_2, *Q* presented in an previous paper of authors [13].

Acknowledgements

The authors gratefully acknowledge the financial supports from the Natural Sciences and Engineering Research Council (NSERC) of Canada and Ontario Centres of Excellence (OCE). Thanks also go to Hibbit, Karlsson and Sorensen, Inc. for making ABAQUS available under an academic licence to Carleton University.

References

[1] J.W. Hutchinson, Singular behaviour at the end of a tensile crack in a hardening material. *Journal of the Mechanics and Physics of Solids*, Vol. 16 (1968) 13–31.

[2] J. R. Rice, G.F. Rosengren, Plane strain deformation near a crack tip in a power law hardening material. *Journal of the Mechanics and Physics of Solids*, Vol. 16 (1968) 1–12.

[3] J.R. Rice, A path independent integral and the approximate analysis of strain concentration by notches and cracks. *Journal of Applied Mechanics*, Vol. 35 (1968) 379–386.

[4] C. Betegon, J.W. Hancock, Two parameter characterization of elastic-plastic crack-tip fields. *Journal of Applied Mechanics*, Vol. 58 (1991) 104–110.

[5] A.M. Al-Ani, J.W. Hancock, *J*-dominance of short cracks in tension and bending. *Journal of the Mechanics and Physics of Solids*, Vol. 39 (1991) 23–43.

[6] Z.Z. Du, J.W. Hancock, The effect of non-singular stress on crack-tip constraint. *Journal of the Mechanics and Physics of Solids*, Vol. 39 (1991) 555–567.

[7] N.P. O'Dowd, C.F. Shih, Family of crack-tip fields characterized by a triaxiality parameter – I. Structure of fields. *Journal of the Mechanics and Physics of Solids*, Vol. 39 (1991) 989–1015.

[8] N.P. O'Dowd, C.F. Shih, Family of crack-tip fields characterized by a triaxiality parameter – II. Fracture applications. *Journal of the Mechanics and Physics of Solids*, Vol. 40 (1992) 939–963.

[9] S. Yang, Higher order asymptotic crack tip fields in a power-law hardening material, Ph.D. Dissertation, University of South Carolina, USA, 1993.

[10] S. Yang, Y.J. Chao, M.A. Sutton, Higher-order asymptotic fields in a power-law hardening material. *Engineering Fracture Mechanics*, Vol. 45 (1993) 1–20.

[11] G.P. Nikishkov, An algorithm and a computer program for the three-term asymptotic expansion of elastic-plastic crack tip stress and displacement fields. *Engineering Fracture Mechanics*, Vol. 50 (1995) 65–83.

[12] G.P. Nikishkov, A. Bruckner-Foit, D. Munz, Calculation of the second fracture parameter for finite cracked bodies using a three-term elastic-plastic asymptotic expansion. *Engineering Fracture Mechanics*, Vol. 52 (1995) 685–701.

[13] P. Ding, X. Wang, Solutions of the second elastic-plastic fracture mechanics parameter in test specimens. *Engineering Fracture Mechanics*, Vol. 77 (2010) 3462-3480.

[14] P. Ding, X. Wang, An estimation method for the determination of the second elastic-plastic fracture mechanics parameters. *Engineering Fracture Mechanics*, Vol. 79 (2012) 295-311.

[15] O. Pop, M. Méité, F. Dubois, J. Absi, Identification algorithm for fracture parameters by combining DIC and FEM approaches. *International Journal of Fracture*, Vol. 170 (2011) 101–114.

[16] M. Méité, O. Pop, F. Dubois, J. Absi, Characterization of mixed-mode fracture based on a complementary analysis by means of full-field optical and finite element approaches. *International Journal of Fracture*, Vol. 180 (2013) 41–52.

[17] B. Moran, C.F. Shih, A general treatment of crack tip contour integrals. *International Journal of Fracture*, Vol. 35 (1987) 295-310.

[18] ABAQUS Manual, Version 6.6, Hibbitt, Karlsson & Sorensen, Inc., Pawtucket, RI, 2006.

[19] N.P. O'Dowd, O. Kolednik, V.P. Naumenko, Elastic-plastic analysis of biaxially loaded center -cracked plates. *International Journal of Solids and Structures*, Vol. 36 (1999) 5639-5661.

[20] Y.J. Chao, X.K. Zhu, *J*-A_2 characterization of crack-tip fields: Extent of *J*-A_2 dominance and size requirements. *International Journal of Fracture*, Vol. 89 (1998) 285–307.